Pathways of Polymeric Vesicle Formation

Giuseppe Battaglia*

Department of Engineering Materials, The Kroto Research Institute, The University of Sheffield, Broad Lane, Sheffield S3 7HQ, U.K.

Anthony J. Ryan

Department of Chemistry, Dainton Building, The University of Sheffield, Brook Hill, Sheffield S3 7HF, U.K.

Received: February 3, 2006; In Final Form: April 7, 2006

Polymeric vesicle formation is dictated by the mutual diffusion of water into the bulk block copolymer and vice versa. The hydration of three poly(ethylene oxide)-*co*-poly(butylene oxide) copolymers with different molecular weights has been monitored both macroscopically (confocal laser scanning microscopy) and microscopically (small-angle X-ray scattering). Both methods have revealed that the amphiphilic block copolymers swell in water following two qualitatively different growth regimes. Initially, water and copolymer diffuse into each other following a subdiffusional growth as the result of a molecular-level arrangement of the amphiphilic membranes that comprise the swollen copolymer. After a critical time, which is exponential in polymer molecular weight, the amphiphilic membranes reach their equilibrium morphology and as a consequence the growth starts to follow Fickian diffusion. The complex hydration kinetics dictate the phases formed at the interface between the amphiphilic copolymer and water. Upon hydration of simple amphiphiles, the amphiphilic film swells and the concentration gradient at the interface with water gradually drops to zero. This strongly affects the complex driving forces that control vesicle formation. Indeed, to form vesicles, an energy barrier has to be overcome, and therefore a constant concentration gradient is required. We show, by enhancing the hydration kinetics via an ac field, how the interface concentration gradient is kept constant and the magnitude of this gradient dictates the final size of the vesicles.

Introduction

Recent progress in polymer physics and chemistry has facilitated the design and the synthesis of "super" amphiphilic membranes made by self-assembly of block copolymers.[1] Their longer chains make these polymer amphiphiles assemble into entangled polymer membranes with enhanced stability and improved mechanical properties compared to the analogous biological membranes.[2,3] Several examples of block copolymeric vesicles (dispersed spherical enclosed membranes) have been reported[1,4] with different chemistry and functionalities with a range of potential applications extending from traditional delivery systems[5,6] to electronics.[7]

Amphiphilic membranes, as well as other supramolecular entities such as micelles, are the result of the balance of forces arising respectively from the interaction between water and the hydrophobic and the hydrophilic parts that comprise the amphiphile.[8−11] These interactions are strongly dependent on temperature and concentration. As a general rule, amphiphiles assemble in water into long-ranged order lyotropic phases at high concentration and into dispersed isotropic supramolecular structures at low concentration. In membrane-forming amphiphiles, the transition from lyotropic to isotropic coincides with the passage from connected membranes, lyotropic lamellae stacks, to disconnected membranes, that is, vesicles.[12] As the water content increases, the lamellae swell to a point where the balance of hydrophilic and hydrophobic forces changes and the membranes rearrange to nonplanar configurations.[13] This is, generally, known as membrane unbinding,[13−15] and it is controlled by the thermal fluctuations of the membrane. The magnitude of such fluctuations depends on the stiffness and the molecular properties of the membrane, and they will, of course, decide the fate of the unbound structures. In recent studies[16,17] performed on membrane-forming poly(ethylene oxide)-poly-(butylene oxide) (EB) block copolymers, the evolution of morphologies formed at different copolymer concentrations in water has been mapped as a function of the copolymer molecular weight. The hierarchy of pseudoequilibrium structures has been observed to strongly depend on the size of the amphiphile. In Figure 1, the different phase sequences are shown schematically as a function of concentration in water and molecular weight. EB copolymers form inverse hexagonal structures at high concentration, and as the water content decreases, the hexagonal structures evolve into lamellar gels. The size, and, therefore, the molecular weight, of the amphiphile strongly affects the mechanical properties of the membrane and, in particular, its stiffness.[18] This implies that the unbinding transition results in the formation of sponge phases and different lyotropic−isotropic transitions as a function of the molecular weight. In the case of high molecular weight copolymers, the mainly disordered sponge phase has been found to break into gel clusters made of close-packed unilamellar vesicles,[16] whereas at low molecular weight structures comprising vesicles interconnected by tubules have been observed.[17] Both morphologies, eventually, break up into vesicle dispersions at very low concentration in water.

Such transitions have very complex kinetics and are governed by the mutual diffusion of amphiphile into water and water into

* To whom correspondence should be addressed. Fax: +440114 222 5943. E-mail: g.battaglia@sheffield.ac.uk.

10.1021/jp060728n CCC: $33.50
Published on Web 05/11/2006

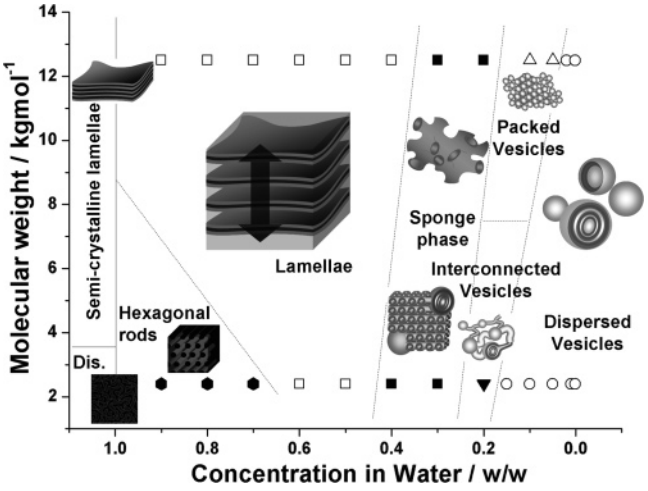

Figure 1. EB copolymer morphologies formed in water as a function of concentration and molecular weight (redrawn from ref 17).

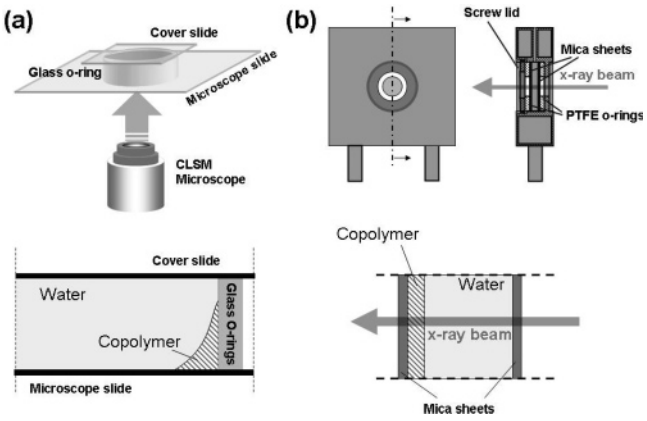

Figure 2. Experimental setup for monitoring the copolymer hydration kinetics by (a) confocal laser scanning microscopy and (b) small-angle X-ray scattering.

the amphiphile. Membrane-forming amphiphiles have, however, a very low critical aggregate concentration.[19] Furthermore, this concentration is almost zero for high molecular weight block copolymers. Polymeric amphiphiles have, therefore, very slow chain exchange, implying that they assemble into locally isolated, nonergodic strucutres.[20−22] Consequently amphiphile diffusion does not occur as single molecules but as the collective diffusion of such nonergodic assemblies. At the same time, as the water diffuses into the bulk amphiphile, the structure of these assemblies rearranges as a function of the local water−amphiphile ratio (Figure 1). The architecture of such structures will obviously have a drastic effect on the hydrodynamics and the diffusion throughout hydration. These complex kinetics result in the formation of metastable structures, usually referred to as kinetic instabilities[23] at the interface water−amphiphile. One of the most frequently encountered is the formation of multilamellar tubular structures known as myelins.[23−26]

In vesicle preparation protocols the contact between water and amphiphile can be achieved in two different ways: phase inversion and organic solvent free techniques. In the former the amphiphile is first dissolved in a organic solvent, and then solvent is more or less gradually exchanged by water, either by evaporation[27,28] or dialysis.[29−31] These methods are based on variation of the packing parameters and therefore on the optimal surface area per molecule, it is often possible to observe the transition from micelle to vesicles as a function of the ratio of organic solvent to water.[32,33] While the size and the morphologies of the final vesicles can be efficiently controlled, the final membrane will always contain a considerable amount of organic solvent, which can limit the application of such systems for biomedical purposes. In organic solvent free conditions, the amphiphile is first deposited onto a surface and then hydrated in the presence of an energy source such as mixing[34] or ac electrical field.[35,36] All these different techniques have shown the formation of unilamellar vesicles with a size that changes considerably from one technique to another. Electroformation of vesicles from polymeric film deposited onto electrodes,[35,36] and phase inversion[28] from chloroform amphiphile solutions, for example, results in the formation of micrometer-sized vesicles, while rehydration techniques[34] such as vigorous mixing with water, sonication,[34] or extrusion,[37] have all been reported to give more or less polydisperse nanosize vesicles. Furthermore, the size distribution can be controlled and narrowed by sonication[34] or extrusion.[37] Herein the different vesicle formation pathways are analyzed by studying the formation of polymeric vesicles from poly(ethylene oxide)-*co*-poly(butylene oxide). At first the kinetics of hydration are studied in detail and modeled using a generalized random walk approach. Subsequently, the formation of vesicles is monitored in the presence of an ac electrical field and compared with the formation in simple hydration. Using an analogy with crystallization, the final vesicle size is derived to be strongly dependent on the concentration gradient.

Experimental Section

Materials. $E_{16}B_{22}$ (M_W = 2300), $E_{50}B_{70}$ (M_W = 7300), and $E_{115}B_{103}$ (M_W = 12 500) copolymers were prepared by sequential anionic copolymerization. Molecular weight and structure were calculated by gel permeation chromatography and ^{13}C NMR as described elsewhere.[38] Rhodamine B octadecyl ester perchlorate amphiphilic fluorescent dye and chloroform were supplied by Aldrich-Sigma Ltd.

Confocal Laser Scanning Microscopy. Confocal laser scanning microscopy was performed using a Zeiss LSM 510M. Copolymer vesicle formation was imaged in the presence of a small amount (0.1−0.2% w/w$_{copolymer}$) of rhodamine B octadecyl ester perchlorate. Z-stack images with *z*-thickness of 200 μm were collected at intervals of 2 min for the first 2 h and 10 min for the subsequent 3 h. Ortho-normal plane images and 3D projections were obtained by image analysis performed by Zeiss LSM image analyzer version 3.2.0.70.

Small X-ray Scattering. Small-angle X-ray scattering (SAXS) experiments were performed on beam line 6.2 of the Synchrotron Radiation Source (SRS) at the Daresbury Laboratory, Warrington, U.K. The beam line is configured for SAXS experiments using monochromatic radiation with beam size of 0.5 mm and wavelength[39] λ = 1.4 Å. SAXS data were collected at an interval of 0.5 min for 2 h and 10 min for the subsequent 3 h.

Hydration Kinetics. EB copolymers and rhodamine B octadecyl ester perchlorate (0.1−0.2% w/w$_{copolymer}$) were first dissolved in chloroform at a concentration of 4 mg/mL. For the confocal laser scanning microscopy measurements, a glass O-ring was immersed in a solution of copolymer in chloroform and placed in a vacuum oven overnight. The glass O-ring was then mounted onto a microscope slide. Water was added into the O-ring, and the top was sealed by a glass cover slip (Figure 2a). The copolymer swelling, $L(t)$, was calculated at different hydration times as the average value measured from the glass support to the first structure observed at the interface with water using four different focus positions. For scattering measure-

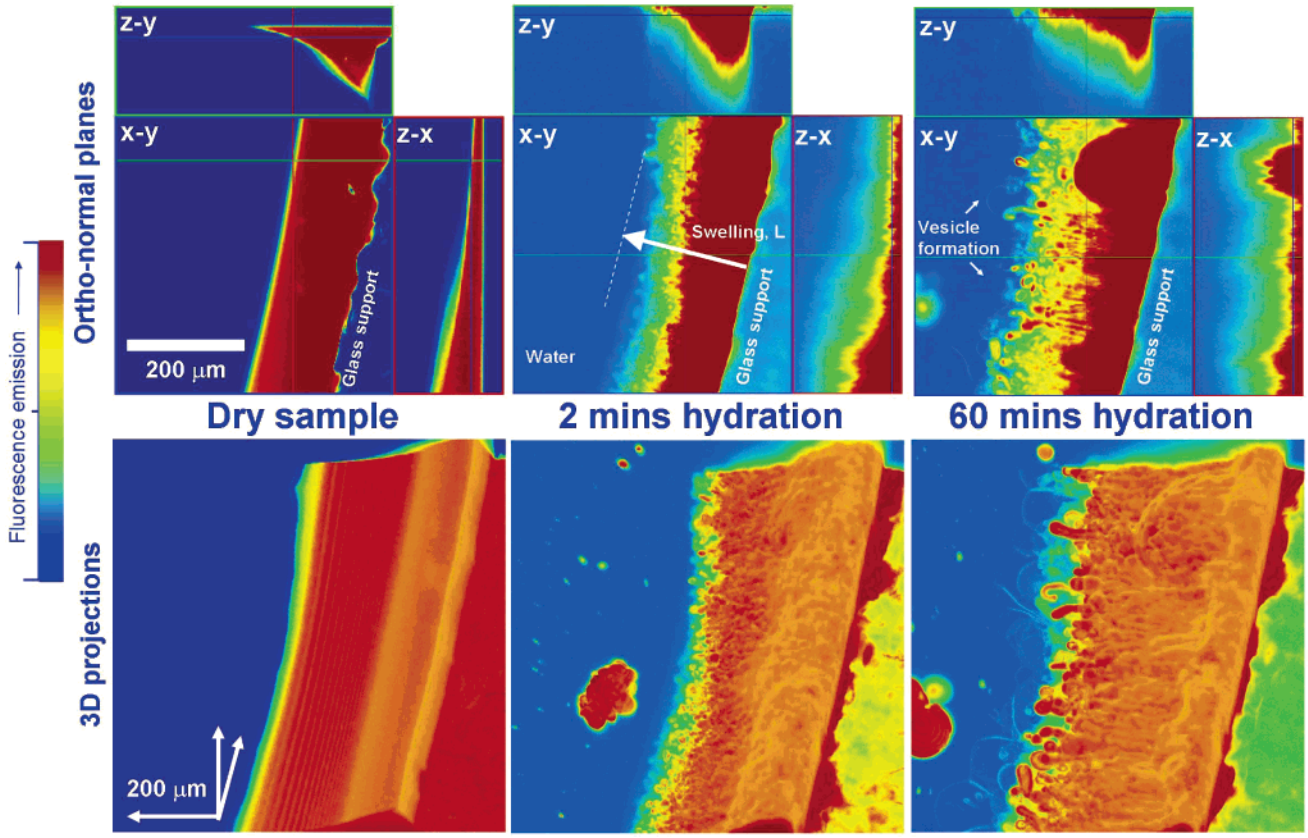

Figure 3. $E_{16}B_{22}$ hydration kinetics monitored by time-resolved confocal laser scanning micrographs at different focus positions. The micrographs are then added up into both ortho-normal planes and 3D projections.

ments, the copolymer is deposited, in a similar way but using a mica sheet rather than a glass slide. This was then immersed in water and sealed. The experimental setup is shown schematically in Figure 2b. The X-ray beam passes through the whole copolymer thickness, which was measured by microscopy to be approximately 300 μm. In both cases, the ratio water/copolymer is made such to have a final concentration of copolymer of 0.5% (w/w) in water. At this concentration all the block copolymers studied have been previously reported[2] to form stable vesicles.

Electroformation. EB copolymers were first dissolved in chloroform at a concentration of 4 mg/mL. Two platinum bars ($20 \times 5 \times 2$ mm) are immersed into the solution and placed in a vacuum oven. The copolymer deposits onto the bars by the evaporation of chloroform. The bars are successively placed onto a microscope slide, immersed into distilled water at a distance of 0.5 cm, and connected to an alternating current (ac) electrical field generator.[36] The ac electrical field was applied at a frequency of 10 Hz and at 10 V.

Results and Discussion

Amphiphilic Copolymer Hydration Kinetics. We have identified (Figure 1), for the most part, the pseudoequilibrium morphological behavior of EB copolymers in water.[16,17] The kinetics of hydration and diffusional processes that take place in the membrane-forming EB copolymers hydration have been studied herein by confocal laser scanning microscopy (CLSM) and small-angle X-ray scattering for three different EB block copolymers: $E_{16}B_{22}$ ($M_W = 2300$), $E_{50}B_{70}$ ($M_W = 7300$), and $E_{115}B_{103}$ ($M_W = 12\,500$) (where the subscripts to E and B refer to the weight average degree of polymerization of ethylene oxide and butylene oxide respectively).

In Figure 3 the hydration and consequent swelling of $E_{16}B_{22}$ is shown by CLSM micrographs at different times and at different focus positions in the film. The addition of water causes the upper layer of copolymer to swell and its surface to wrinkle, forming finger instabilities known as myelins. It has been previously demonstrated[24] that EB myelins can grow to great length (up to millimeters), but, if left in excess water, they will eventually destabilize and form vesicles. The EB hydration and its consequent swelling are governed by the mutual diffusion of the water in the copolymer and the copolymer assembly into water. In his original work on Brownian motion, Einstein[40] derived his diffusion equation using the random walk model, by supposing that the direction of motion of a particle gets "forgotten" after a certain time, and the mean-squared displacement during this time is finite (the squared displacements have a Gaussian distribution). Assuming, therefore, that the motion of different particles is independent, there exists a time interval, t^*, such that the displacements of the same particle during different t^* intervals can be considered to be independent, and there is a mean-squared $\langle x^2(t)\rangle$ displacement of the particle during such a t^* interval. The mean-squared displacement can be written as

$$\langle x^2(t)\rangle \sim Kt \tag{1}$$

While this approach is valid for the majority of the diffusional process, it fails to describe the diffusional process in several systems.[41] In these cases, the overall motion of an object is better described by steps that are not independent and take considerable time to occur. Such diffusion processes no longer follow Gaussian statistics, and thus Fick's second law fails to describe the related transport behavior. This can be expressed as deviations from the linear time dependence of the mean-squared

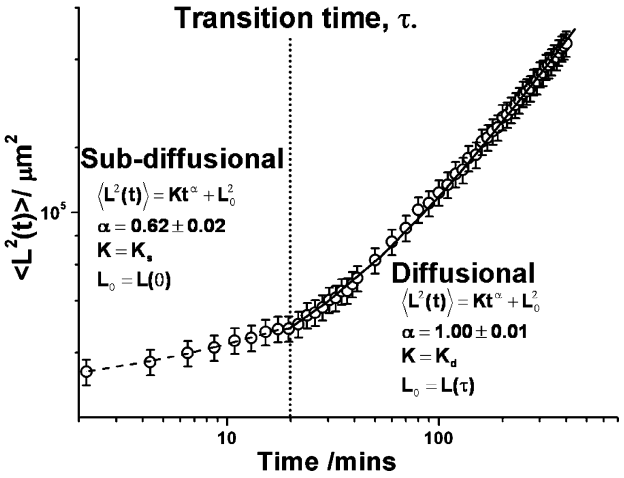

Figure 4. Macroscopic swelling of $E_{16}B_{22}$ plotted versus time. The copolymer swells initially following a subdiffusional growth, and, after a certain time, defined as the transition time, τ, the swelling starts to follow a normal diffusional growth.

displacement. A more generalized approach rests on the validity of the Levy−Gnedenko generalized central limit theorem,[42] and a power law can be applied in order to describe diffusional phenomena.

$$\langle x^2(t)\rangle \sim K_\alpha t^\alpha \tag{2}$$

According to the value of the diffusion exponent, α, several regimes of anomalous transport can be distinguished. When $\alpha = 1$, the transport phenomena follow a Brownian diffusion regime; when $\alpha > 1$, a superdiffusional regime; and when $0 < \alpha < 1$, a subdiffusional regime. Particularly, the latter regime is characterized[43] by a time dependence of the mean square displacement of a particle. In physical terms, such anomalous diffusion is related to the infinitely long, average time that an object undertaking a random walk waits to make a finite jump. In other words, the random walker pauses between steps and there are large steps or long periods in which there is no motion. This phenomenon has been previously reported for diffusion phenomena such as diffusion in porous media[44] and charge carrier transport in amorphous semiconductors[45] and in fluctuating protein systems.[46]

Accordingly herein, the mutual diffusion of copolymer in water and vice versa can be studied by measuring the overall swelling of the amphiphilic copolymer in water, $L(t)$ (Figure 3). This can be considered as the mean displacement of a random walk, and its time course can thus be generalized as

$$\langle L^2(t)\rangle = K_\alpha t^\alpha + L_0{}^2 \tag{3}$$

If the exponent α is unity, the squared swelling $\langle L^2(t)\rangle$ is linear with t, and the swelling follows a normal (Brownian) diffusion. When α is not unity, the distributions of summed random variables are too broad or the variables are correlated; thus the swelling follows an anomalous diffusion pathway.

The macroscopic swelling, $L(t)$, has been monitored from CLSM micrographs (Figure 3) at different times and focus positions. The swelling is measured from the glass support to the water as an average value over different focus heights. The graph in Figure 4 is a time course of the squared swelling $\langle L^{2(t)}\rangle$. The experimental data have been fitted using eq 3. The initial mutual diffusion of water and amphiphilic copolymer has been found to follow a subdiffusional trend with exponent $\alpha = 0.62$. After a certain time, which has been defined as the *transition time*, τ, there is a qualitative change in the swelling behavior and it starts to follow a normal diffusional growth ($\alpha = 1$). The two different diffusional regimes can be rationalized on the basis of morphological changes due to the variation of the water content with time. As the water diffuses into the amphiphilic copolymer, the balance between hydrophilic and hydrophobic interactions changes, leading to the formation of different structures. The water diffuses in at a faster rate than the copolymer diffuses out, causing a moving interface (swelling). The phase sequence of EB copolymers as a function of concentration in water, from rods to lamellae, through to a sponge phase and finally to isolated vesicles (Figure 1) is contained within the thickness of the film, which is typically 200−500 μm. Under simple hydration conditions, the hydrodynamics of the system is only controlled by the mutual diffusion of water in the copolymer and fully swollen lamellar phases in water. Consequently, the local fluid dynamics are dramatically different as a function of position in the interfacial region.

To understand such molecular-level changes, the thickness-averaged structure of the copolymer, during hydration, has been analyzed as a function of time by SAXS. In Figure 5a the SAXS patterns of swollen $E_{16}B_{22}$ are presented as a function of hydration time. The X-ray beam passes through the full thickness of the film (Figure 1b); i.e., the measured SAXS pattern is a weighted average of all the structures present. In the bulk $E_{16}B_{22}$ is disordered and the scattering is a small peak due to density fluctuations;[17] but as soon as water is added to this polymer, intense scattering peaks can be observed due to the formation of a highly ordered morphology. The water is a preferential solvent for E, and hydrated E is more incompatible with the B block. The water sequesters within the E domains, and the complex SAXS patterns that arise are the consequence of a gradient of water through the copolymer and the sequence of phases that form as a function of concentration. The first phase formed[17] by $E_{16}B_{22}$ on dilution with water is hexagonally packed rods, and at concentrations between 70 and 60% (w/w) the hexagonal phase transforms into a lamellar phase. However, the intense peak present in the first few minutes corresponds to a d spacing of a lamellar gel formed by $E_{16}B_{22}$ at about 60% (w/w) polymer in water. This indicates that either the hexagonal−lamellae transition is very fast (and is missed even in the short time scales of the synchrotron SAXS experiment) or that it does not occur at all.

The time course of the d spacing ($d = 2\pi/q^*$) and the peak intensity at $q = q^*$ are plotted in Figure 5b, the d spacing reaches a plateau after 20 min, ascribed to the unbinding of lamellae.[17] The peak intensity also shows two distinct regimes with a change in behavior after 20 min. This time scale is exactly the transition between subdiffusional and diffusional swelling. The final d spacing lamellar gel corresponds to a concentration of less than 50% (w/w) polymer. At this concentration, under pseudoequilibrium conditions the same copolymer was reported to have a transition from lamellae to sponge phase, typical of unbinding membranes. As the water content increases, the intensity of the peak decreases and the SAXS pattern becomes dominated by form factor scattering typical of multilamellar and unilamellar aggregates.[17] SAXS data have, thus, revealed that as water diffuses into the copolymer film, a number of morphological transitions take place. The diffusion of water into a homogeneous disordered block copolymer is qualitatively different from the diffusion of water into a minority hexagonal phase and different again from the diffusion of water into alternating hydrophobic and hydrophilic lamellae. The complex,

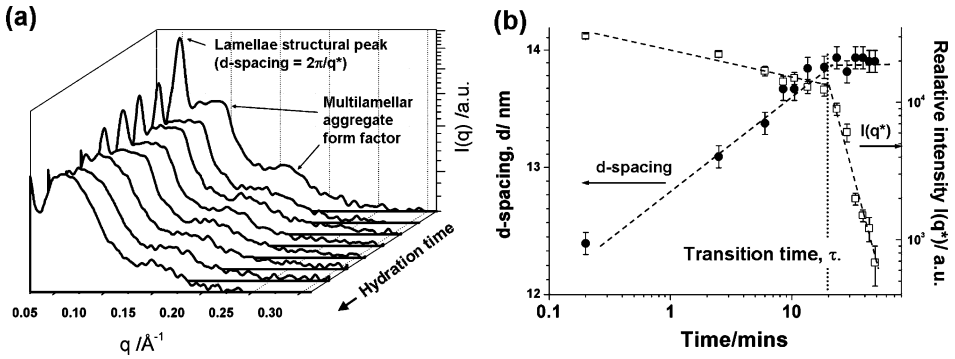

Figure 5. (a) SAXS patterns of the swelling $E_{16}B_{22}$ copolymer at different hydration times. (b) Lamellae *d* spacing and the intensity of the diffraction peak over time.

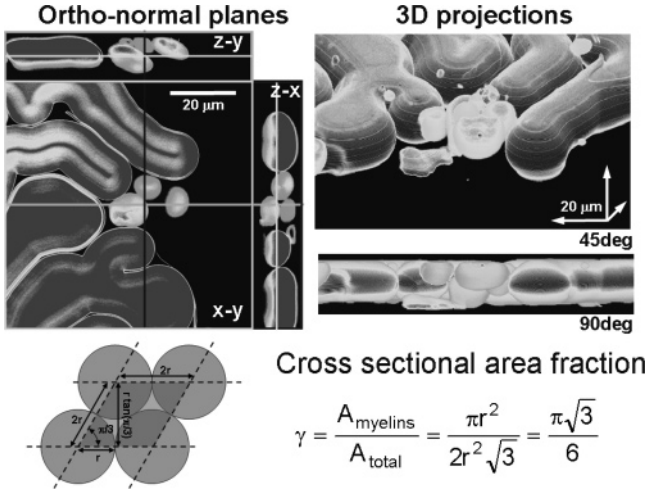

Figure 6. Magnification of the myelins formed at the interface copolymer−water. To a first approximation, the myelins can be considered to be close-packed, and the cross-sectional area fraction is calculated accordingly.

time-dependent SAXS data are convolutions of water diffusing into the film with all three phases (melt, rods, and lamellae) present.

Using the generalized random walk approach, the initial diffusion of water into the copolymer can be thought to occur through pauses between the random walk steps, and there are large steps or long periods in which there is no motion. These periods are necessary for allowing the different rods−lamellae−vesicle transitions to take place as the water content increases. Consequently, the initial growth of the copolymer follows a subdiffusional regime.

Once all the lamellae are unbound or almost unbound, no more phase transitions take place, and consequently the swelling of the amphiphilic copolymer is only dependent on the mutual diffusion of the water and the copolymer in each other. The copolymer swelling can be therefore derived from eq 3 with exponent $\alpha = 1$:

$$L(t) = k_p\sqrt{t-\tau} + L(\tau) \tag{4}$$

where k_p is a proportionality constant related to the diffusion velocity and $L(\tau)$ is the swelling value corresponding to τ. As already reported[24] and visible in the CLSM micrographs in Figure 6, the copolymer evolves from bulk to water via the formation of myelins. In Figure 6, the $z-x$ ortho-normal plane and the 3D projection calculated at 90° show that the myelins are close-packed together. To a first approximation, the cross-sectional area fraction can be, therefore, calculated as $\gamma = \pi\sqrt{3}/6 = 0.907$, as shown in Figure 6. This assumption has been confirmed experimentally by monitoring both myelin growth and water permeation in swelling lamellar phases.[26] By invoking the conservation of mass, the copolymer flux from bulk to water can be calculated as

$$J_p(t) = \gamma\frac{dL(t)}{dt} = \frac{k_p}{2\sqrt{t-\tau}} \tag{5}$$

At $t = \tau$ and therefore at $L(t) = L(\tau)$, the diffusion process can be rationalized, in first approximation, using the first Fick's law. Assuming that the concentration gradient is $dC(t)/dx \approx \Delta C/L(t) \approx 1/(L(t) - L(\tau))$ and according to eq 4, the copolymer flux can be expressed as

$$J_p(t) = D_{coll}\frac{dC(t)}{dx} \cong D_{coll}\frac{1}{L(t)-L(\tau)} = D_{coll}\frac{1}{k_p\sqrt{t-\tau}} \tag{6}$$

where D_{coll} is the collective diffusion coefficient of water into copolymer and copolymer into water; this value can be therefore derived by combining eqs 5 and 6:

$$D_{coll} \cong \gamma\frac{k_p^2}{2} \tag{7}$$

The collective diffusion coefficient calculated for the smallest molecular weight, $E_{16}B_{22}$, ($D_{coll} = 1.03 \times 10^{-13}$ m^2 s^{-1}) is 3 orders of magnitude smaller than the value reported for the nonionic surfactant triethylene glycol monotridecyl ether ($C_{12}E_3$) in water ($D_{coll} = 8.5 \times 10^{-11}$ m^2 s^{-1}).[26] The difference is obviously due to the fact that $E_{16}B_{22}$ has a higher molecular weight (2300 g/mol), and hence lower mobility, than the nonionic surfactant (318 g/mol).

The effect of molecular weight on the diffusion process can be observed from the graph in Figure 7a, where the squared swellings of three different molecular weight EB copolymers are presented. The time axis is normalized with respect to τ, and the swelling is normalized by its value at that time $L^2(\tau)$ and the dry copolymer thickness $L^2(0)$. The initial subdiffusional behavior appears to be universal in all of the three different molecular weight copolymers as the normalized data fall on the same master curve. This confirms that the initial anomalous diffusional behavior is mainly due to morphological arrangements of the copolymers as a function of water concentration. Once the final equilibrium structure is formed, the lamellar copolymer grows according to normal diffusion. At this point, higher molecular weight and therefore more viscous copolymers have slower diffusion. As a result, the collective diffusion coefficient drops almost 3 orders of magnitudes in only 1 order

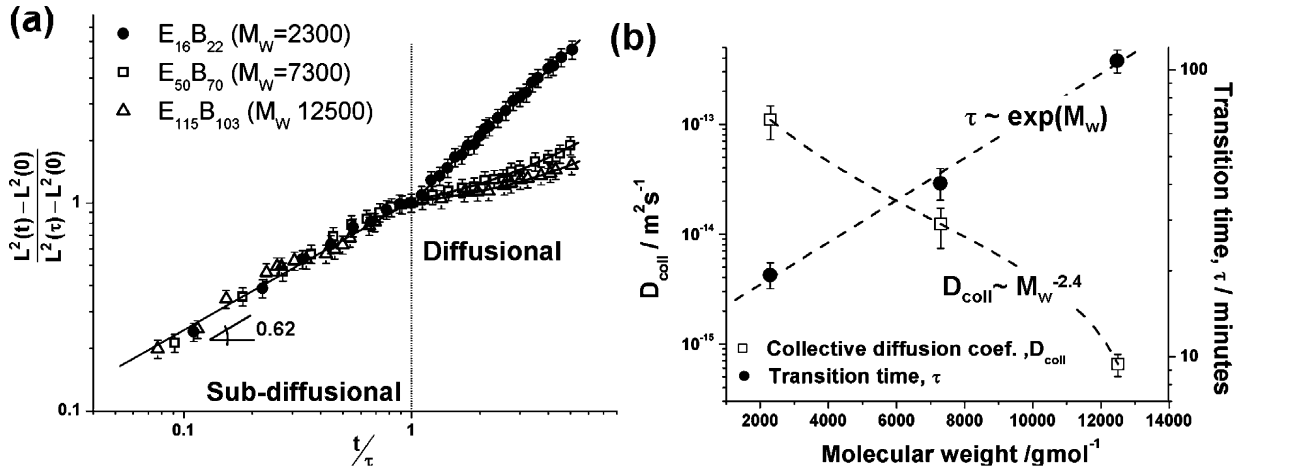

Figure 7. (a) Time course of the swelling process. The time axis is normalized with respect to the transition time, τ, and the swelling is normalized by its value at that time and the initial layer thickness. (b) Collective diffusion coefficients and the transition times as a function of the molecular weight. The transition times fit in an exponential function, while the collective diffusion coefficients have been fitted with a power law $D_{coll} \sim Mw^{-2.4}$.

of magnitude of molecular weight (Figure 7b), the three data indicate a power law for diffusion as $D \sim M_w^{-2.4}$, and a similar result was reported for bulk copolymers by Tao et al.[47] In addition, the transition time changes exponentially as a function of the molecular weight, suggesting sub-diffusional regimes that last longer as the molecular weight increases: this is a direct result of much slower kinetics of swelling, phase transitions and membrane unbinding.

Vesicle Formation. Consider for simplicity vesicle formation under solvent-free conditions, at the interface between copolymer and water the two assembling driving forces are the diffusion of the copolymer in water and the diffusion of the water in the copolymer. Given two different amphiphile concentrations at the copolymer front C_0 and at the water front C_1, the concentration gradient can be defined as $\Delta C = C_1 - C_0$.

The concentration gradient depends on the mutual diffusion of the water into the copolymer and the nonergodic copolymer−water aggregates into the water. In all the vesicle formation protocols under solvent-free conditions, the contact between water and amphiphiles occurs with the supply of energy; by mechanical mixing or by application of an ac electrical field on the interface, the mutual diffusion is enhanced. The lyotropic lamellae swell and very soon are placed under conditions of complete and drastic unbinding; the amphiphilic membranes have therefore all the time necessary to evolve into the most stable structure.

In Figure 8, different confocal laser scanning micrographs show the formation of vesicles from $E_{16}B_{22}$ with and without an additional energy input (ac electrical field). In simple hydration conditions, the amphiphilic membranes swell forming myelin figures at the interface with water in the first 30 min. This moving interface has a strong effect on the concentration gradient. This can be estimated by the difference of relative fluorescence emission at two extremes over time. Under simple hydration, as shown in Figure 8, the concentration gradient decreases almost linearly with time. As the concentration gradient changes, the lamellar structures do not have sufficient time to unbind completely. This leads the formation of myelins at the interfaces which eventually evolve into vesicles.[24] These vesicles are visible at the interface copolymer/water after 1 h, although, the majority of them do not complete their vesiculation and do not detach from the interface.

In contrast, when additional energy is supplied to the system, the diffusion, of the copolymer into water and/or the diffusion of water into the copolymer is strongly enhanced. This leads to a fast and complete formation of vesicles, which then detach from the interface. Consequently, the amphiphile does not swell because most of the material is eroded in the form of vesicles. In other words, the concentration gradient at the amphiphile−water interface is kept constant. This can also be observed in Figure 8, where EB vesicle formation has been monitored under the application of an ac electrical field. As described in the Experimental Section, the copolymer is deposited onto a platinum electrode. Such protocol, known as vesicle electroformation has been intensively used for the generation of micrometer-sized vesicles.[36] It is commonly accepted that vesicle formation occurs via the electrostatic movement of the water at the water−electrode interface. These vibrations are directed perpendicular to the electrode surface and facilitate both the water diffusion into the amphiphile and the lamellae-membrane unbinding. It has also been previously demonstrated that the electrical field can generate forces that prevail over the surface tension in liquid−liquid and polymer−air interfaces. [48,49] This means that the transition time is practically zero and the collective diffusion coefficient is highly enhanced. As shown in Figure 8, this results in a stable copolymer−water interface and consequently a constant concentration gradient.

The concentration gradient can be considered to be the driving force for vesicle formation; consequently, it plays a very crucial role in determining the vesicle final size. In analogy with crystallization, the amphiphile membrane can be thought of as the unit cell and the vesicle as the result of the growth of this cell. The formation of one vesicle can be analyzed in term of the free energy of nucleation. The formation of a sphere with diameter R is driven by a negative free energy of volume and opposed by a positive interfacial energy. The two contributions will make up the total free energy of formation as follows:

$$\Delta G = -\frac{4}{3}\pi R^3 \Delta\mu + 4\pi R^2 \gamma \qquad (8)$$

where γ is the interfacial energy and $\Delta\mu$ is the difference of the chemical potential from the bulk state to the vesicle. This value depends strictly on the ratio of concentrations of the amphiphile-rich film and the dilute solution of amphiphile. In the case of electroformation the copolymer film rapidly reaches

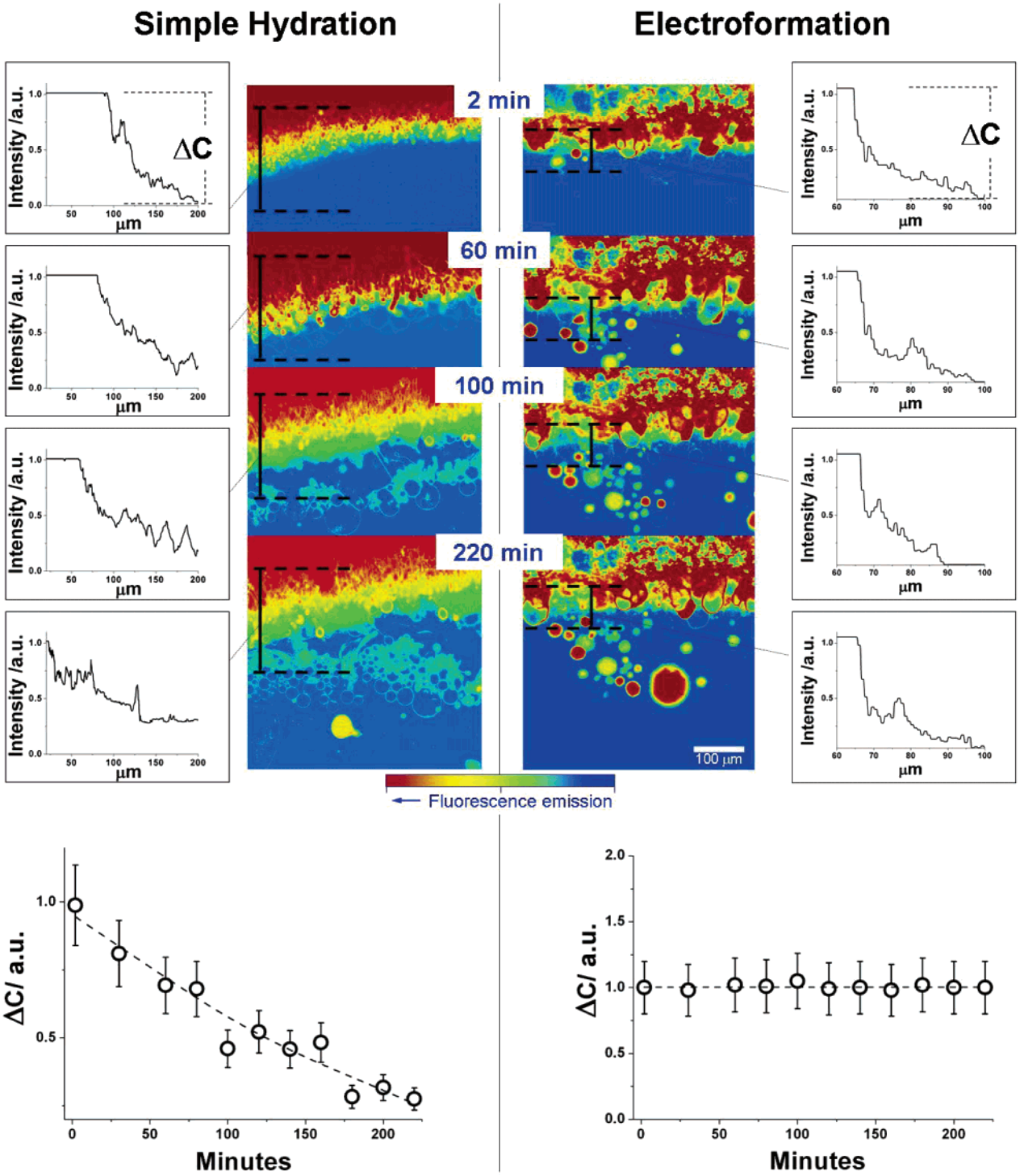

Figure 8. CLSM micrographs to illustrate the temporal evolution of the $E_{16}B_{22}$−water interface in the case of simple hydration and electroformation. The concentration gradient at the interface can be estimated by both the color gradient and the florescence emission one-dimensional profile. The concentration gradient is calculated as the difference between the extreme in the profiles, and its temporal evolution is shown in the graphs below.

the pseudoequilibrium unbinding concentration, whereas in other methods the film or the polymer particles have the bulk copolymer concentration. The chemical potential difference driving the formation of vesicles is logarithmic in the concentration ratio $\Delta\mu \sim \ln(C_1/C_0)$. Equation 8 will have a maximum at $R^* = 2\gamma/\Delta\mu$, and in crystallization theory this is known as the critical size above which the crystalline nuclei will grow into bigger crystals. The critical value is inversely proportional to the difference of chemical potential and therefore to the concentration gradient, $R^* \approx 2\gamma/\ln(C_1/C_0)$. Thus under conditions of mixing and rehydration the logarithmic term will be larger and the vesicles will have diameter on the order of nanometers, while, in the presence of a mild diffusion enhancer, such as an ac electrical field, the vesicles are growing from a lower copolymer concentration and will grow to be very large with a final diameter on the order of decades of micrometers. This explanation of how the electric field overcomes the kinetic barrier to vesicle formation, through enhanced diffusion of water into the bulk film and amplification of the fluctuations at the free interface, suggests that not only is the kinetic barrier overcome but also that the final vesicle size might be tunable through the electric field strength.

Conclusions

The hydration and the consequent swelling of vesicle-forming E_mB_n copolymers is dominated by the balance between attractive and repulsive forces that arise from the respective interactions between hydrophobic and hydrophilic blocks with water. Such balance is strongly dependent on the water−copolymer ratio and therefore on the diffusion of the water through the copolymer and vice versa. At concentrations between 100 and 40% (w/w), the copolymers have been found[16,17] to form different lyotropic phases, and therefore the initial swelling is controlled not only by the mutual diffusion of water and copolymer but also by the phase transitions that take place such as hexagonal rods to lamellae and the subsequent membrane unbinding. Using a generalized random walk approach, the initial swelling can be interpreted as an anomalous diffusion and particularly as a subdiffusional growth.[43] The time when the subdiffusional regime ends and a normal diffusional regime starts has also been found to coincide with the time where the lyotropic lamellae start to unbind as showed by monitoring the lamellae *d* spacing and the intensity of the structural peak. The process of vesicle formation by diffusion of water in a membrane-forming block copolymer highlights some unusual physics. The initial subdiffusional regime, clearly observed here, corresponds to the series of phase transitions leading to the lamellae and the elimination of grain boundaries. Once the lamellae start to unbind, normal diffusion mechanisms are operand. This result not only demonstrates the complex kinetics of amphiphile hydration but also presents a novel natural phenomenon with anomalous diffusional processes and provides a model system to study diffusion-induced phase transitions and their effect on the global diffusion process. These kinetics studies have also uncovered the fact that in order to form polymer vesicles a constant concentration gradient is required at the interface between copolymer and water. The variation of such gradient resolves in the formation of metastable structures, such as multilamellar aggregates, which might have very long life due to the nonergodic nature[21,22] of amphiphilic membranes and the slow kinetics of destabilization intrinsic of macromolecular systems. The effect of the concentration gradient has been analyzed in detail, comparing vesicle formation in simple hydration conditions with those where additional energy is supplied (ac electrical field). This kinetic barrier has also been demonstrated to dictate the final size of vesicles using crystal growth arguments.

Acknowledgment. The authors would like to thank Dr. Shao-min Mai for the synthesis of the EB copolymers and the ICI Strategic Technology Group for financial support.

References and Notes

(1) Discher, D. E.; Eisenberg, A. *Science* **2002**, *297*, 967.
(2) Battaglia, G.; Ryan, A. J. *J. Am. Chem. Soc.* **2005**, *127*, 8757.
(3) Discher, B. M.; Won, Y.-Y.; Ege, D. S.; Lee, J. C.-M.; Bates, F. S.; Discher, D. E.; Hammer, D. A. *Science* **1999**, *284*, 1143.
(4) Antonietti, M.; Förster, S. *Adv. Mater.* **2003**, *15*, 1323.
(5) Ahmed, F.; Discher, D. E. *J. Controlled Release* **2004**, *96*, 37.
(6) Ghoroghchian, P. P.; Frail, P. R.; Susumu, K.; Blessington, D.; Brannan, A. K.; Bates, F. S.; Chance, B.; Hammer, D. A.; Therien, M. J. *Proc. Natl. Acad. Sci. U.S.A.* **2005**, *102*, 2922.
(7) Stanish, I.; Lowy, D. A.; Hung, C.-W.; Singh, A. *Adv. Mater.* **2005**, *17*, 1194.
(8) Israelachvili, J. N.; Wennerstrom, H. *Nature* **1996**, *379*, 219.
(9) Israelachvili, J. N. *Intermolecular and Surface Forces*, 9th ed.; Elsevier Science Imprint: London, 2002.
(10) Tanford, C. *Hydrophobic Effect: Formation of Micelles and Biological Membranes*, 1st ed.; John Wiley & Sons: New York, 1973.
(11) Tanford, C. *Proc. Natl. Acad. Sci. U.S.A.* **1979**, *76*, 4175.
(12) Helfrich, W. *J. Phys.: Condens. Matter* **1994**, *6*, A79.
(13) Lipowsky, R. *Nature* **1991**, *349*, 475.
(14) Lipowsky, R.; Leibler, S. *Phys. Rev. Lett.* **1986**, *56*, 2541.
(15) Leibler, S.; Lipowsky, R. *Phys. Rev. B* **1987**, *35*, 7004.
(16) Battaglia, G.; Ryan, A. J. *Nat. Mater.* **2005**, *4*, 869−876.
(17) Battaglia, G.; Ryan, A. J. *Macromolecules* **2006**, *39*, 798.
(18) Bermudez, H.; Brannan, A. K.; Hammer, D. A.; Bates, F. S.; Discher, D. E. *Macromolecules* **2002**, *35*, 8203.
(19) Israelachivili, J. N. *Intermolecular and Surface Forces*, 9th ed.; Elsevier Science Imprint: London, 2002.
(20) Won, Y.-Y.; Davis, H. T.; Bates, F. S. *Macromolecules* **2003**, *36*, 953.
(21) Jain, S.; Bates, F. S. *Science* **2003**, *300*, 460.
(22) Jain, S.; Bates, F. S. *Macromolecules* **2004**, *37*, 1511.
(23) Buchanan, M.; Starrs, L.; Egelhaaf, S. U.; Cates, M. E. *Phys. Rev. E* **2000**, *62*, 6895.
(24) Battaglia, G.; Ryan, A. J. *Angew. Chem., Int. Ed.* **2006**, *45*, 2052.
(25) Buchanan, M.; Arrault, J.; Cates, M. E. *Langmuir* **1998**, *14*, 7371.
(26) Buchanan, M.; Egelhaaf, S. U.; Cates, M. E. *Langmuir* **2000**, *16*, 3718.
(27) Szoka, F.; Papahadjopoulos, D. *Proc. Natl. Acad. Sci. U.S.A.* **1978**, *75*, 4194.
(28) Moscho, A.; Orwar, O.; Chiu, D. T.; Modi, B. P.; Zare, R. N. *Proc. Natl. Acad. Sci. U.S.A.* **1996**, *93*, 11443.
(29) Kabanov, A. V.; Bronich, T. K.; Kabanov, V. A.; Yu, K.; Eisenberg, A. *J. Am. Chem. Soc.* **1998**, *120*, 9941.
(30) Luo, L.; Eisenberg, A. *Langmuir* **2001**, *17*, 6804.
(31) Luo, L.; Eisenberg, A. *J. Am. Chem. Soc.* **2001**, *123*, 1012.
(32) Choucair, A.; Eisenberg, A. *Eur. Phys. J. E* **2003**, *10*, 37.
(33) Shen, H.; Eisenberg, A. *J. Phys. Chem. B* **1999**, *103*, 9473.
(34) Gregoriadis, G. *Preparation of Liposomes*; CRC Press: Boca Raton, FL, 1984.
(35) Angelova, M. I.; Dimitrov, D. S. *Faraday Discuss.* **1986**, *81*, 303.
(36) Menger, F. M.; Angelova, M. I. *Acc. Chem. Res.* **1998**, 789.
(37) Olson, F.; Hunt, C. A.; Szoka, F. C.; Vail, W. J.; Papahadjopoulos, D. *Biochim. Biophys. Acta* **1979**, *9*, 557.
(38) Ryan, A. J.; Mai, S.-M.; Fairclough, J. P. A.; Hamley, I. W.; Booth, C. *Phys. Chem. Chem. Phys.* **2001**, *3*, 2961.
(39) Cernik, R. J.; Barnes, P.; Greaves, G. N.; Rayment, T.; Ryan, A. J. *Appl. Crystallogr.* **2004**, *19*, 3.
(40) Einstein, A. *Ann. Phys. (Berlin)* **1906**, *19*, 371.
(41) Metzler, R.; Klafter, J. *J. Phys. A: Math. Gen.* **2004**, *37*, R161−R208.
(42) Bouchaud, J.-P.; Georges, A. *Phys. Rep.* **1990**, *195*, 127.
(43) Metzler, R.; Klafter, J. *Phys. Rep.* **2000**, *339*, 1.
(44) Wong, I. Y.; Gardel, M. L.; Reichman, D. R.; Weeks, R. E.; Valentine, M. T.; Bausch, A. R.; Weitz, A. D. *Phys. Rev. Lett.* **2004**, *92*, 1781011.
(45) Scher, H.; Montroll, E. W. *Phys. Rev. B* **1975**, *12*, 2455.
(46) Min, W.; Luo, G.; Cherayil, B. J.; Kou, S. C.; Xie, X. S. *Phys. Rev. Lett.* **2005**, *94*, 1983021.
(47) Tao, H.; Lodge, T. P.; Meerwall, E. D. v. *Macromolecules* **2000**, *33*, 1747.
(48) Schäffer, E.; Thurn-Albrecht, T.; Russell, T. P.; Steiner, U. *Nature* **2000**, *403*, 874.
(49) Lin, Z.; Kerle, T.; Baker, S. M.; Hoagland, D. A.; Schäffer, E.; Steiner, U.; Russell, T. P. *J. Chem. Phys.* **2001**, *114*, 2377.